Available online at www.sciencedirect.com
SCIENCE DIRECT®
Journal of Sound and Vibration 279 (2005) 993–1014
JOURNAL OF SOUND AND VIBRATION
www.elsevier.com/locate/jsvi

In-plane dynamic behavior of cable networks. Part 2: prototype prediction and validation

L. Caracoglia, N.P. Jones*

Department of Civil and Environmental Engineering, University of Illinois, Urbana, IL 61801, USA

Received 20 December 2001; accepted 25 November 2003

Abstract

An analytically based and numerically implemented method for the prediction of the behavior of cable networks has been developed for the analysis of the in-plane free-vibration problem of a set of interconnected taut cable elements. The methodology has been extended to large systems with complex configurations and applied to the study of the oscillation mitigation of a real case on an existing cable-stayed bridge.

Validation of the model has been performed through the comparison of the predictions with experimental data derived from an extended ambient survey on an actual structural system. In addition, the study includes a sensitivity analysis related to the introduction of design modifications to the original configuration. The observations deduced from this research have contributed to the definition of preliminary criteria for the selection of an optimized system.

1. Introduction

A companion paper [1] describes the methodology for the analytical derivation of the equation of motion associated with the in-plane free-vibration problem of a cable network with a reduced number of elements and a simple connection; closed-form solutions of these cases were also presented.

The original procedure is extended herein to consider the in-plane modal analysis of large cable networks. The problem of non-parallel orientation of the cables (three dimensional) and non-orthogonal patterns of the grid (cables and restrainers) and the influence of the stiffness on the transverse connectors is addressed.

*Corresponding author. Tel.: +1-217-333-9896; fax: +1-217-265-0318.
E-mail address: npjones@uiuc.edu (N.P. Jones).

0022-460X/$ - see front matter © 2003 Elsevier Ltd. All rights reserved.
doi:10.1016/j.jsv.2003.11.059

This methodology is applied to the study of a real case, the Fred Hartman Bridge in Houston, Texas (USA). In the first part of this analysis, the central-span network has been considered; the modes of the existing system are computed and, subsequently, a sensitivity analysis is carried out by introducing some modifications to the original design (locations and number of restrainers, ground connections). The knowledge of the basic solutions [1] is used for the interpretation and the identification of similar behavior also for a large system with several stays. In the second part, the side-span arrangement is considered and the modal analysis is compared to experimental results derived from an intensive ambient vibration survey of the same bridge that is currently in progress [2,3].

2. Extension of the original methodology to large cable networks

2.1. Generalization of the problem for orthogonal-grid systems

The extension of the procedure, presented in Section 2 of Ref. [1] for a perfectly orthogonal grid, is depicted in Fig. 1. The generic jth cable ($j = 1, \ldots, n$) is divided into m_j segments due to the presence of the transverse cross-ties. The quantities $m_1, \ldots, m_j, \ldots, m_n$ are different for each cable to account for a generalized configuration of the network with a variable number of connectors (and segments) on each stay.

The jth cable is restrained at both ends. The geometric and physical characteristics of the jth cable are indicated as: length L_j, tension H_j and mass per unit length μ_j. The upper stay of the network ($j = 1$, Fig. 1) is considered as reference. The remaining quantities are normalized with respect to this element, i.e.,

$$\omega_{01} = \frac{\pi}{L_1}\left(\frac{H_1}{\mu_1}\right)^{1/2}, \quad f_j = \frac{\omega_{01}}{\omega_{0j}} = \frac{f_{01}}{f_{0j}}, \quad v_j = \left(\frac{\mu_j H_j}{\mu_1 H_1}\right)^{1/2}, \tag{1–3}$$

where ω_{01} is the fundamental circular frequency of the upper (usually longest) cable, ($f_{0j} = \omega_{0j}/2\pi$); f_j is defined as the generic jth cable frequency ratio and v_j as a mass–tension reduction

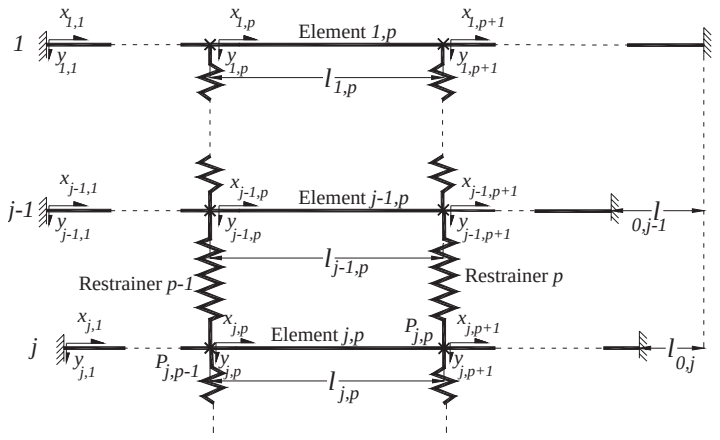

Fig. 1. Generalized system of interconnected cables (orthogonal elements).

factor. The length of the pth segment of the jth cable, the limits of which are defined by the nodes $P_{j;p-1}$ and $P_{j;p}$, is denoted as $l_{j,p}$ (with $p = 1, \ldots, m_j$); accordingly, its reduced length, defined as the ratio of the individual element length over the length of the corresponding jth cable is $\xi_{j,p} = l_{j,p}/L_j$.

The horizontal offset between the jth stay with respect to the reference cable is indicated as l_{Oj} ($l_{O1} = 0$). The pth cross-tie (Fig. 1) is simulated by means of spring vertical elements with generic stiffness $K_{j,p}$, with $j = 1, \ldots, g_p$, where $g_p \leqslant n$ is the number of connected cables, for the pth connector.

The x_{jp} along-axis co-ordinate of the pth segment of the jth cable (with $j = 1, \ldots, n$; $p = 1, \ldots, m_j$) has been taken in accordance with Fig. 1; transverse displacements, $y_{jp}(x_{jp}, t)$, where t denotes the time variable, are considered positive downwards. The free-vibration problem is concerned with the solution of a system of r partial differential equations (see Eq. (1) of Ref. [1], with $j = 1, \ldots, n$ and $p = 1, \ldots, m_j$), in which $y_{jp}(x_{jp}, t) = Y_{jp}(x_{jp})\mathrm{e}^{i\omega t}$; ω is the natural circular frequency of the coupled network (unknown), Y_{jp} are appropriate spatial-dependent functions, and $r = \sum_{j=1}^{n} m_j$ is the total number of elements.

This problem can be reduced to a system of ordinary equations (see Eq. (3) of Ref. [1]). The generalized form of the $Y_{j,p}$ functions can be proposed as

$$Y_{j,p}(x_{j,p}) = A_{j,p} \sin\left(\frac{\alpha\pi}{L_j} f_j x_{j,p}\right) + B_{j,p} \cos\left(\frac{\alpha\pi}{L_j} f_j x_{j,p}\right), \tag{4}$$

where $\alpha = \omega/\omega_{01} = f/f_{01}$ is the reduced (dimensionless) frequency of the network. The $2r$ unknown parameters $A_{j,p}$ and $B_{j,p}$, representing the modal amplitudes of each segment, must be solved from the boundary conditions, which are given by the continuity and compatibility set of equations (equivalent to Eqs. (2), (A.2) and (A.4) in Ref. [1]).

The set of compatibility, continuity, equilibrium expressions for a cable network can be generalized (after simplification of the $\mathrm{e}^{i\omega t}$ terms) as

$$B_{j,1} = 0 \quad \text{with } j = 1, \ldots n, \tag{5}$$

$$A_{j,m_j} \sin(\alpha\pi f_j \xi_{j,m_j}) + B_{j,m_j} \cos(\alpha\pi f_j \xi_{j,m_j}) = 0 \quad \text{with } j = 1, \ldots n, \tag{6}$$

$$A_{j,p_j} \sin(\alpha\pi f_j \xi_{j,p_j}) + B_{j,p_j} \cos(\alpha\pi f_j \xi_{j,p_j}) - B_{j,p_j+1} = 0 \tag{7}$$

with $j = 1, \ldots n$, $p_j = 1, \ldots, m_j$,

$$K_{j,p}(B_{j+1,p+1} - B_{j,p+1}) = \sum_{k=1}^{j} \frac{\alpha\pi H_1}{L_1} \sigma_{k,j}^{p} v_k \{A_{k,p} \cos(\alpha\pi f_k \xi_{k,p}) - B_{k,p} \sin(\alpha\pi f_k \xi_{k,p}) - A_{k,p+1}\} \tag{8}$$

with $p = 1, \ldots, \tilde{m} - 1$, $j = 1, \ldots, (g_p - 1)$, $\tilde{m} = \max[g_p]$,

$$K_{G_p} B_{g_p,p+1} = \sum_{j=1}^{g_p} \frac{\alpha\pi H_1}{L_1} \sigma_{j,g_p}^{p} v_j \{A_{j,p} \cos(\alpha\pi f_j \xi_{j,p}) - B_{j,p} \sin(\alpha\pi f_j \xi_{j,p}) - A_{j,p+1}\} \quad \text{with } p = 1, \ldots, \tilde{m} - 1. \tag{9}$$

Eqs. (5) and (6) represent the condition of vertical displacement vanishing at each stay end, Eq. (7) the along-cable internal continuity of displacement between two consecutive segments p and $p+1$. Eq. (8) state the transverse internal continuity between points $P_{j,p}$ and $P_{j+1,p}$, by taking into account the transverse force equilibrium of the upper part of the network (Fig. 2(a)) and the elongation of the spring element, with stiffness $K_{j,p}$, interconnecting the two stays and equivalent to the relative vertical displacement between nodes $P_{j,p}$ and $P_{j+1,p}$. Expressions (9) summarize the vertical global force equilibrium at each cross-tie location, by considering an eventual spring-to-ground connection with stiffness K_{G_p} (Fig. 2(b)). The quantities $\sigma_{k,j}^{p}$ in Eqs. (8) and (9) are identically equal to one for a perfectly orthogonal grid (details will be given in Section 2.2).

It can be shown that the set of expressions (5)–(9) define the $2r$ compatibility equations required by system (2) in Ref. [1]. The solution to the free-oscillation problem, and the determination of the natural frequencies in terms of α, can be transformed into a system $\mathbf{S}$ of algebraic equations, by assembling together Eqs. (5)–(9), in a more compact matrix form

$$\mathbf{S\Phi} = \mathbf{0}, \tag{10}$$

$$\mathbf{\Phi}[2r \times 1] = [A_1 \ \cdots \ A_q \ \cdots \ A_r; \quad B_1 \ \cdots \ B_q \ \cdots \ B_r]^{\mathrm{T}}, \tag{11}$$

where vector (8), $\mathbf{\Phi}$, regroups all the unknowns as A_q and B_{q+r}, corresponding to a given element j,p, in terms of a unifying parameter q, such that $A_q = A_{j,p} B_{q+r} = B_{j,p}$.

The infinite set of non-trivial solutions ($\mathbf{\Phi} \neq \mathbf{0}$) of the homogeneous system (10), associated with the condition $\det[\mathbf{S}] = 0$, can be solved as an equivalent eigenvalue/eigenvector problem, related to the transcendental nature of expressions (5)–(9), in which the solution, corresponding to the free-vibration analysis, is sought in terms of the reduced frequency α. The set of α-solutions cannot be generally identified in closed form for a complex structure; a numerical iterative procedure is employed for the solution of the characteristic polynomial related to $\det[\mathbf{S}] = 0$. For

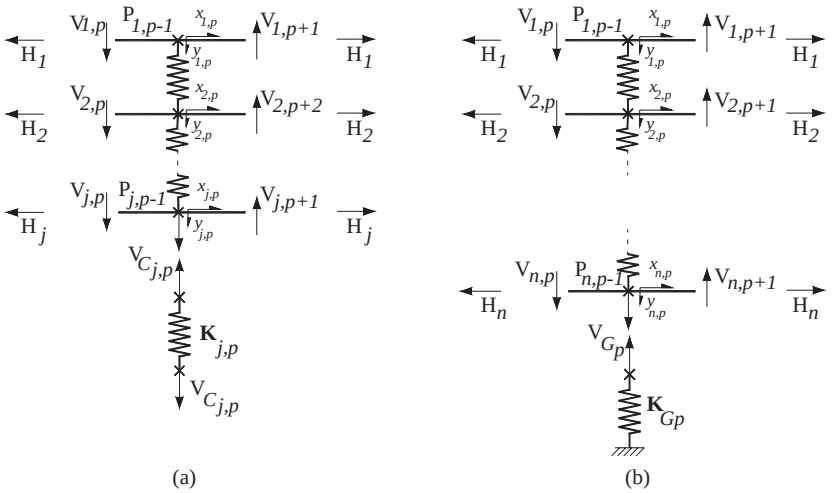

Fig. 2. Compatibility conditions corresponding to (a) internal vertical continuity (10,12) and (b) global equilibrium at each connector location (11,13).

these solutions, α_i, the vector of the modal amplitudes $\mathbf{\Phi}_i$ (A_q and B_{q+r}) is derived from $\mathbf{S}$ along with the corresponding eigenfunctions (4), $Y_{j,p}$, normalized such that

$$\sum_{j=1}^{n}\sum_{p=1}^{m_j}\int_0^{l_{j,p}}\mu_j\left[A_{j,p}\sin\left(\frac{\alpha\pi}{L_j}f_j x_{j,p}\right)+B_{j,p}\cos\left(\frac{\alpha\pi}{L_j}f_j x_{j,p}\right)\right]^2 \mathrm{d}x_{j,p}=1. \tag{12}$$

In addition, the first and second derivatives of the determinant function are numerically computed and compared to det[**S**] in order to evaluate the potential occurrence of multiple solutions associated with the same frequency α as derived in Ref. [1] for particular cases. Multiple eigenvectors related to a given frequency $\tilde{\alpha}$, with $\tilde{\mathbf{S}}=\mathbf{S}(\tilde{\alpha})$, $\det[\tilde{\mathbf{S}}]=0$ and $rank[\tilde{\mathbf{S}}]<2r-1$, can be derived from the eigenvalue problem with complex and multiple eigenvalues:

$$[\tilde{\mathbf{S}}-\tilde{\lambda}\mathbf{I}]\mathbf{\Phi}=\mathbf{0} \tag{13}$$

with $\tilde{\lambda}=0$. Eq. (13), generalization of system (10) for $\alpha=\tilde{\alpha}$, is used in these cases since the iterative numerical computation of $\mathbf{\Phi}$ by a direct solution of system (10) is less efficient.

The method defined by the step-by-step solution of system (10) through the set of compatibility and boundary conditions was applied to the analysis of the relevant examples investigated in Ref. [1], for validation purposes. Very good agreement was obtained with the closed-form solutions previously determined.

2.2. Reduction of three-dimensional networks to equivalent orthogonal-grid systems

A real cable network, in most cases, does not correspond to a perfectly orthogonal grid, since the orientation of the stays (fan system) is usually three dimensional and defined according to cable anchorages at deck and towers [5]. The cables usually lie on a plane that is inclined with respect to the horizontal axis; the slightly imperfect verticality of this plane is neglected in the present analysis.

A set of stays with different in-plane inclination, as simply illustrated in Fig. 3(a) can be reduced to an equivalent parallel taut-strip element by means of a polar-co-ordinate reduction (Fig. 3(b)) with respect to the reference cable (C1 in Fig. 3). Sag effects are neglected in this framework.

The original geometric quantities (length of the segments, position of the restrainers, cable offsets) are redefined in accordance with the parallel orientation (Fig. 3(b)). The local (Fig. 3(b)) displacement variable of the generic "j,p" segment of a perfectly parallel system, $y_{jp}(x_{jp},t)$, can be referred to the real inclined configuration as orthogonal to the cable axis (Fig. 3(a)). The non-parallel orientation of stays and restrainers (three-dimensional force equilibrium) is taken into account through parameters $\sigma_{k,j}^{p}$ in Eqs. (8) and (9) i.e., $\sigma_{k,j}^{p}=\prod_{q=k}^{j-1}(\sin\hat{\psi}_{q,p}/\sin\psi_{q,p})$ (with $\sigma_{j,j}^{p}=1$) where $\psi_{q,p}$ and $\hat{\psi}_{q,p}$ are the relative inclinations between the qth segment of the pth restrainer and the upper (qth) and lower ($(q+1)$th) stay, respectively (e.g., ψ_{11} and $\hat{\psi}_{11}$ in Fig. 3(a)).

Moreover, Eqs. (8) or (9) are referred to a vertical equilibrium (Fig. 2(a) and (b)) through the force $V_{Cj,p}=K_{j,p}\Delta y_{j,p}$ (referred as V_C in Fig. 3(b)), with $\Delta y_{j,p}$ perpendicular relative displacement. The imperfect orthogonal orientation of the generic restrainer in the transformed system ($\psi_{11}\neq\pi/2$ in Fig. 3(b)) with respect to the parallel-cable model can be accounted for by projection of the restoring force and the displacement component in the cross-tie direction.

The internal compatibility equation of an inclined restrainer becomes $F_{Cj,p}=K_{j,p}\delta_{j,p}$, in which both $F_{Cj,p}$ (referred as F_C in Fig. 3(b)) and $\delta_{j,p}$ are taken along the axis of the restrainer, defined

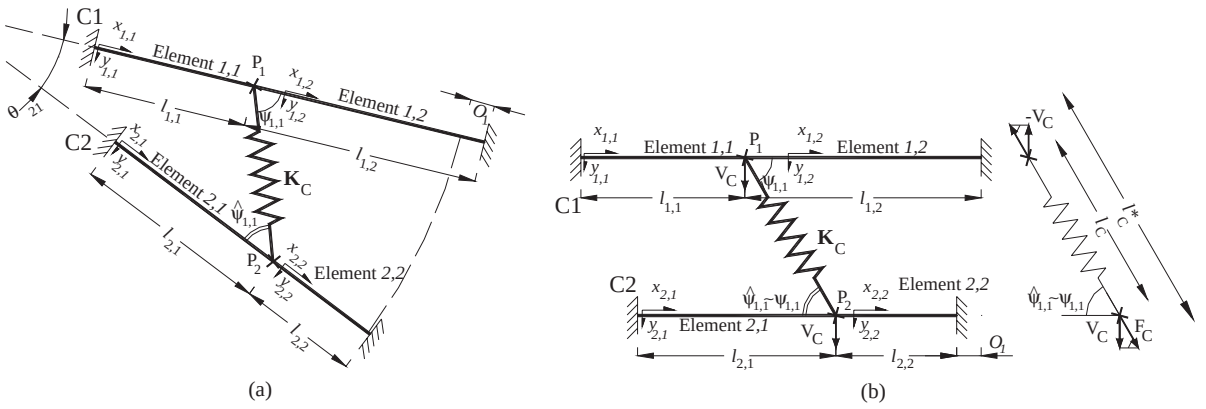

Fig. 3. (a) Inclined-orientation system and (b) polar reduction to parallel stays.

through the inclination $\psi_{j,p}$ between jth cable and pth connector (referred as ψ_{11} in Fig. 3(b), with $\psi_{j,p} \cong \hat{\psi}_{j,p}$). The projection of the force in the perpendicular direction can be written as $V_{Cj,p} = F_{Cj,p} \sin(\psi_{j,p})$, while the effective elongation of the spring $\delta_{j,p}$ (e.g., equal to $l_C^* - l_C$ in Fig. 3(b)) is given by the component of the relative displacement $\Delta y_{j,p}$ between nodes $P_{j;p}$ and $P_{j+1;p}$ ($Y_{P2} - Y_{P1}$ in Fig. 3(b)), in the direction parallel to the restrainer, i.e., $\delta_{j,p} = \Delta y_{j,p} \sin(\psi_{j,p})$. By combining such expressions, an effective stiffness of the inclined cross-tie $K_{j,p}^{EFF}$, to be directly inserted into Eqs. (10) or (11) instead of $K_{j,p}$ can be defined as $K_{j,p}^{EFF} = K_{j,p} [\sin(\psi_{j,p})]^2$.

3. Numerical analysis of the main-span cable network of the Fred Hartman Bridge

The free-vibration analysis method, presented in Section 2 and Ref. [1], was applied to the study of a cable network, modelled after the Fred Hartman Bridge, a twin-deck cable-stayed bridge over the Houston Ship channel, with a central span of 380 m and side spans of 147 m. The deck is composed of precast concrete slabs on steel girders with four lanes of traffic, carried by a total of 192 cables in four inclined planes, connected at 15 m intervals [2,3].

The investigated system corresponds to the south-tower central-span portion, a set of 12 stays ("A-line" from AS13 to AS24) with a three-dimensional arrangement (Fig. 4(a)). The geometric and structural characteristics of the cables are summarized in Table 1(a). Stay "AS24" is assumed as reference element (1–3), with fundamental frequency $f_{01} = 0.617$ Hz.

3.1. Parametric study of the original design of the cable network

The transverse connectors, an "eight-loop" steel wire rope system, are located in accordance with the original design (Fig. 4(a)). The characteristics of these elements are also provided in Table 1(b). The three-dimensional network was reduced to an equivalent two-dimensional problem with parallel elements (Fig. 4(b)) by means of the formulation as in Section 2.2; each cable offset is considered in terms of the inclined system and referred to AS24. The arc configuration of the cross-ties (Fig. 4) was reproduced through equivalent inclined linear spring

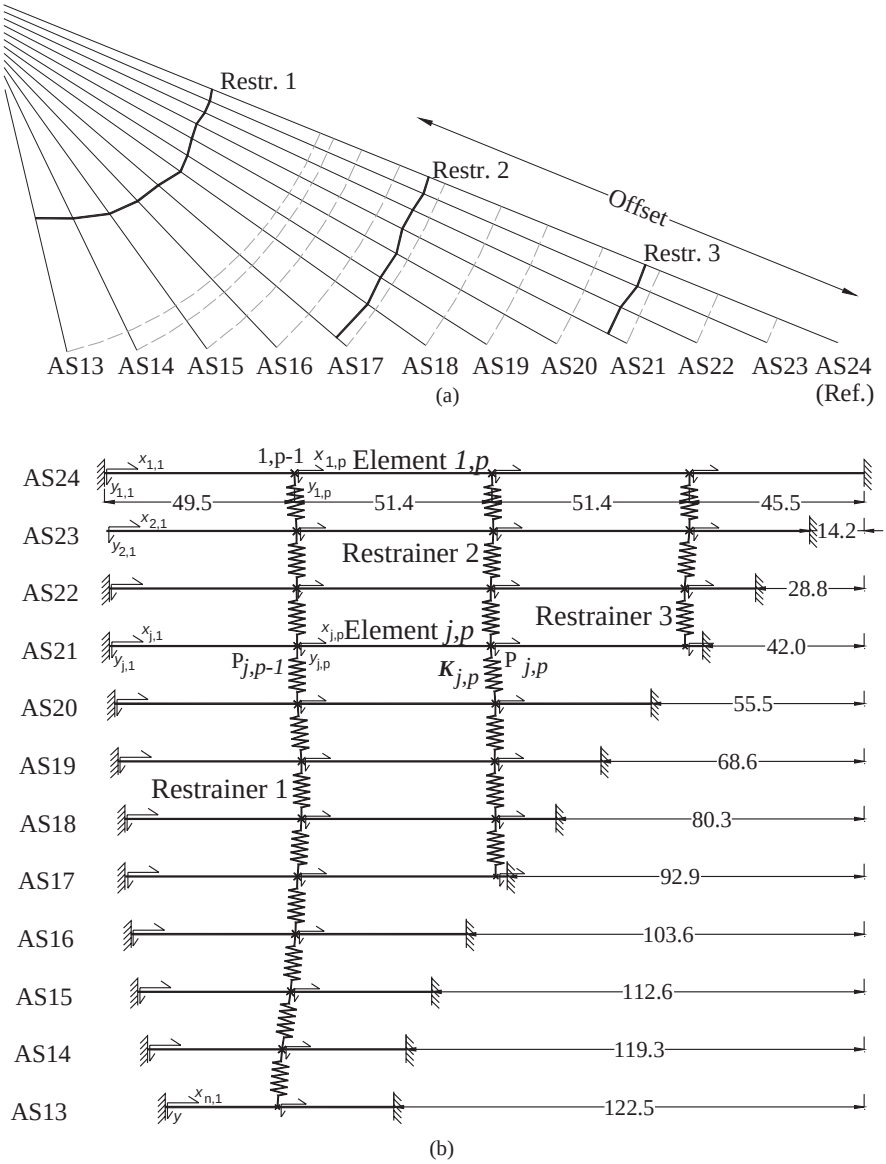

Fig. 4. Main span unit of the Fred Hartman Bridge (“A-line”). (a) Three-dimensional network; (b) equivalent two-dimensional model. Measurements in meters; vertical units are not to-scale.

elements. As a result of this transformation to an equivalent two-dimensional problem, the overall pattern of the model is slightly irregular (Fig. 5), since the lengths of each cable segment were selected at symmetric locations with respect to each stay but not to the global network. The effective normalized stiffness of the inclined connector (25), equivalent to a perfectly orthogonal grid, is also included in Table 1(b).

Fig. 5(a) and (b) depict the evolution of $\det[\mathbf{S}(\alpha)]$ and $(d/d\alpha)\{\det[\mathbf{S}(\alpha)]\}$ in terms of a reduced frequency α. As it can be seen from Fig. 5(a) initial high-amplitude fluctuations with some roots

Table 1
Geometrical and structural characteristics of the Hartman system (central span): (a) stays, (b) restrainers

Stay	Mass (kg/m)	Tension (kN)	L (m)	$L/L_{AS24}(-)$	Freq (Hz)	$f_j(-)$	$v_j(-)$
(a) *Cable-stays*							
AS13	32.5	1651	59.52	0.30	1.89	0.33	0.39
AS14	47.9	1598	67.34	0.34	1.36	0.46	0.47
AS15	47.9	1900	76.55	0.39	1.30	0.47	0.51
AS16	47.9	2158	87.33	0.44	1.21	0.51	0.55
AS17	52.9	2394	99.38	0.50	1.07	0.58	0.61
AS18	52.9	2732	112.28	0.57	1.01	0.61	0.65
AS19	65.2	3204	125.78	0.64	0.88	0.70	0.78
AS20	70.1	3351	139.70	0.71	0.78	0.79	0.83
AS21	70.1	3831	154.08	0.78	0.76	0.81	0.88
AS22	70.1	3547	168.40	0.85	0.67	0.92	0.85
AS23	76.0	4285	183.06	0.93	0.65	0.95	0.97
AS24[a]	76.0	4530	197.85	1.00	0.62	1.00	1.00

Cross-tie segment	Restrainer 1			Restrainer 2			Restrainer 3		
	L (m)	Area (mm^2)	K_{jp}^{Eff} (kN/m) $\times 10^3$	L (m)	Area (mm^2)	K_{jp}^{Eff} (kN/m) $\times 10^3$	L (m)	Area (mm^2)	K_{jp}^{Eff} (kN/m) $\times 10^3$
(b) *Restrainers*									
AS13-14	8.32	570	10.69						
AS14-15	8.05	570	10.65						
AS15-16	6.78	570	14.33						
AS16-17	5.69	570	18.36						
AS17-18	5.74	570	16.25	10.03	570	10.76			
AS18-19	3.84	570	27.95	6.50	570	16.76			
AS19-20	3.86	570	26.88	6.29	570	17.37			
AS20-21	3.34	570	32.12	5.57	570	18.59			
AS21-22	3.05	570	34.80	4.72	570	23.22	6.43	570	17.13
AS22-23	2.78	570	39.61	4.28	570	24.79	5.84	570	17.40
AS23-24	2.64	570	40.11	3.83	570	28.50	5.05	570	21.79

[a] Reference element.

($1<\alpha<3$) are followed by a second interval of reduced frequencies in which the magnitude of the determinant is considerably reduced and a "high-density" set of solutions is present, also shown in the enlargement of Fig. 5(a) and (b) ($3<\alpha<5$). This sequence of "intermittent" amplitude behavior is also repeated in subsequent intervals and for higher modes.

A careful study of these solution patterns showed that the first category of roots are associated with "global modes", in which the whole set of cables is involved in the oscillation, along with a substantial increment in the generalized mass of the mode, with respect to the individual cables. The second category is one of "localized modes", in which the response of network is not global but the maximum amplitudes are located in the intermediate segments of specific cables only.

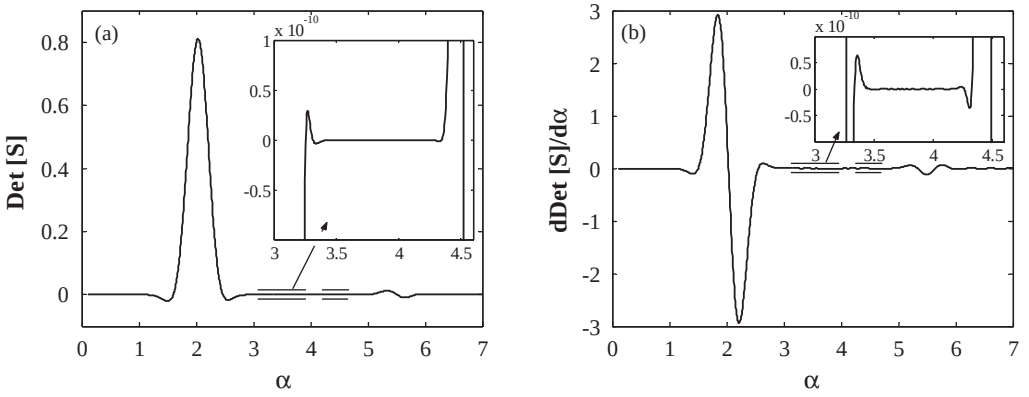

Fig. 5. Central-span unit of the Hartman Bridge (NET_3C). (a) Analysis of the determinant, det[**S**] and (b) its derivative $d/d\alpha$ det[**S**], as a function of the reduced frequency $\alpha = \omega/\omega_{01}$.

Moreover, the overall characteristics of these modal forms can be different from the solution for individual cables, and are influenced by the presence and the location of the transverse connectors. Solutions are antisymmetric or pseudo-symmetric, clearly recalling the behavior highlighted in Section 4 of Ref. [1]. The wavelength of these modes is essentially governed by the distance between two consecutive connectors (being almost coincident with the nodes of the modal shape). The high density of solutions is related to the fact that these modes can be interpreted as the components of high-order modes of the individual cables with different magnitude, for which the location of the connector on each cable represents a potential node associated with the individual-stay mode shape.

Fig. 6 depicts the $Y_r(x_r)$ eigenfunctions of the first eight modes (NM1–NM8) of the two-dimensional model, normalized according to Eq. (21). Indirectly, the chosen representation emphasizes the modal amplitudes of the localized modes (NM4-8) by a high value in the eigenvector component of "internal" elements. The reduced frequency α is also included in Fig. 6, for each solution. Indication of the flexible connectors is provided. Global network modes (1–3), characterized by a reasonable distribution of the modal amplitudes in all the elements, are symmetric and antisymmetric. The subsequent local modes, relatively close in frequency, are associated with a permutation of a similar pattern (e.g., modes 5 and 6) dominated by two or three cables at most, mainly located in the upper part of the network and belonging to the longest cables.

Fig. 7 shows a set of higher modes (27–32) in which the migration from the sequence of highly localized solutions to a second set of global network modes (NM29–32). As the mode number increases, the potential interaction with higher modes of individual cables intensifies, and the distinction between localized and global behavior becomes less evident (e.g., NM32). This characteristic is also suggested by the study of the determinant (Fig. 5), in which a progressive relative-amplitude decrement of the function can be noticed in the frequency interval corresponding to non-localized solutions ($5 < \alpha < 6$).

The importance of the cable bending stiffness on the overall response, not included in the current formulation, may be possibly considered, especially in the case of localized modes for

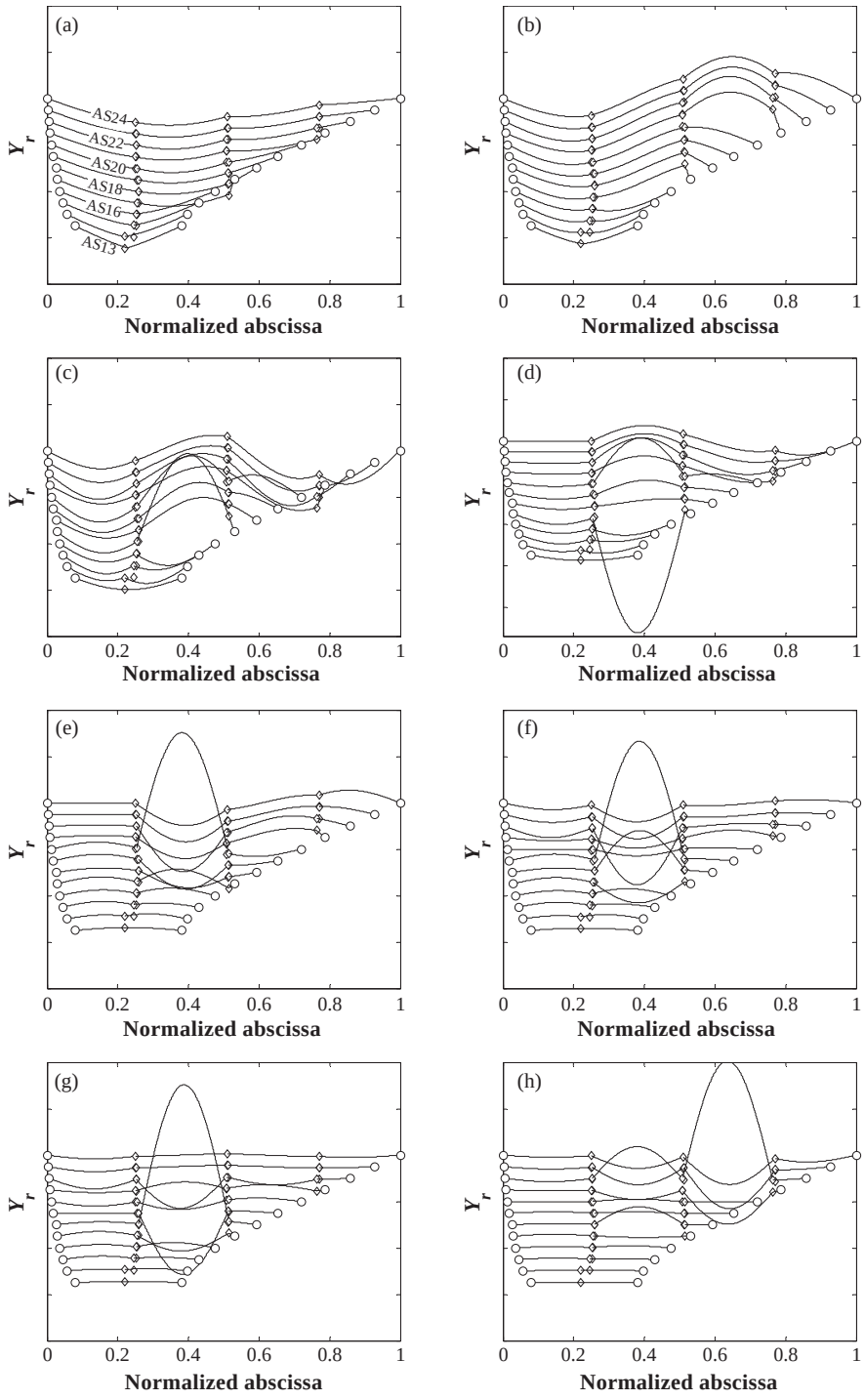

Fig. 6. Central-span unit of the Hartman Bridge (NET_3C); Y_r eigenfunctions associated with the 1–8 network modes (NM1–NM8). (a) NM1, $\alpha = 1.60$; (b) NM2, $\alpha = 2.46$; (c) NM3, $\alpha = 3.26$; (d) NM4, $\alpha = 3.32$; (e) NM5, $\alpha = 3.45$; (f) NM6, $\alpha = 3.54$; (g) NM7, $\alpha = 3.61$; (h) NM8, $\alpha = 3.63$.

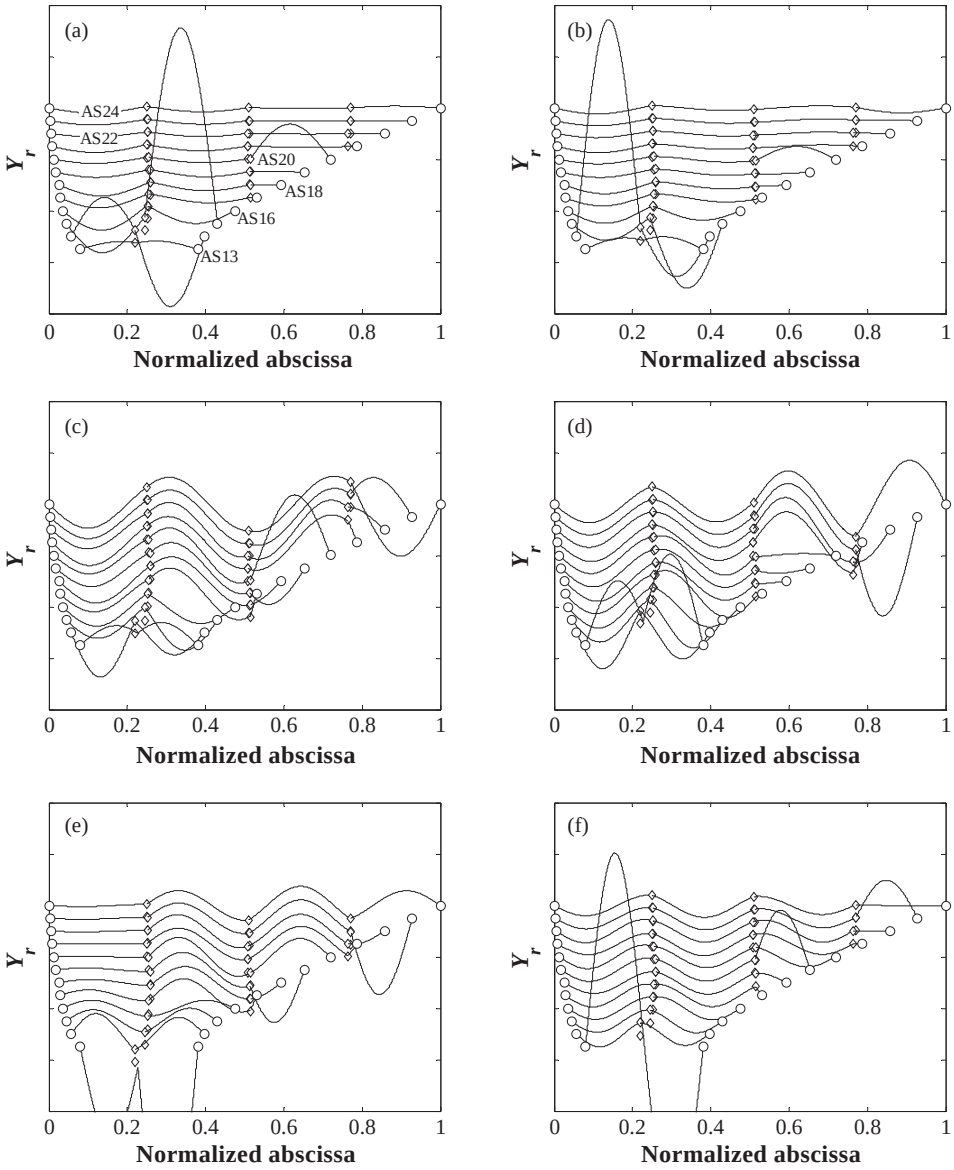

Fig. 7. Central-span unit of the Hartman Bridge (NET_3C); Y_r eigenfunctions associated with higher modes, 27–32 (NM27–NM32). (a) NM27, $\alpha = 4.34$; (b) NM28, $\alpha = 4.52$; (c) NM29, $\alpha = 4.96$; (d) NM30, $\alpha = 5.51$; (e) NM31, $\alpha = 5.84$; (f) NM32, $\alpha = 6.14$.

which the kinking effect, associated with the stay/tie intersection (e.g., Fig. 6 for NM5 and higher, and Fig. 7) would not be physically realizable.

The significance of the connector structural characteristics was evaluated by studying the effect of an increase in their stiffness with respect to the same geometrical configuration. In the first case the simulation of the network with infinitely rigid restrainers was sought; in the second one a

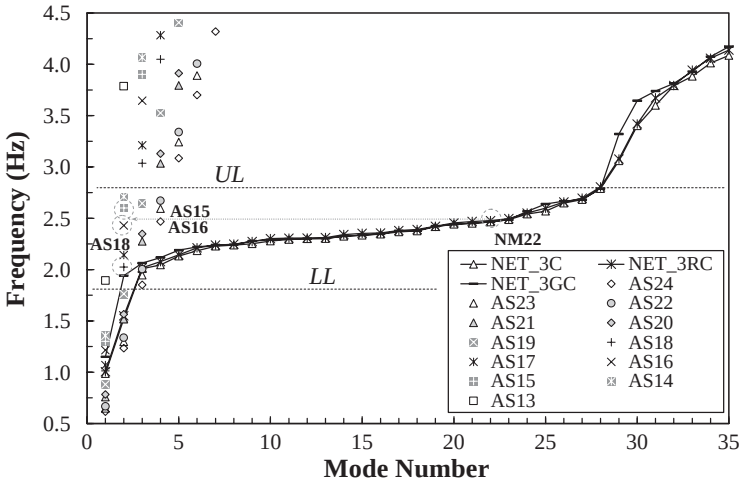

Fig. 8. Mode-frequency evolution curves of the central-span unit of the Fred Hartman Bridge: NET_3C (−△−) original configuration; NET_3RC (−∗−) infinitely rigid restrainers; NET_3CG (- – -) restrainers 2 and 3 extended to ground (*UL* and *LL*, upper and lower limits of the plateau).

system equivalent to Fig. 4(b) with extensions to ground at restrainers 2 and 3 was investigated. Numerical challenges in the resolution of the former case (limiting condition) were carefully addressed.

A comparative study among the three cases (NET_3C, original configuration; NET_3RC simulation of perfectly rigid transverse links; NET_3CG modified non-rigid configuration with ground restrainers) is presented in Fig. 8, in which the natural frequencies (Hz) are plotted as a function of the mode number and compared to the individual cable behavior, also labeled as "mode-frequency evolution chart". A similar representation was introduced by Abdel-Ghaffar and Khalifa [4] for the numerical study of vibration problems of cable-stayed bridges, in which global (deck, towers) and local modes were identified.

From this figure, the structural behavior can be efficiently and graphically characterized: the sequence of fundamental global modes associated with large modal masses (between 0.9 and 2 Hz) is followed by a typical plateau with high density of solutions, corresponding to the localized modes with considerably lower modal mass, governed by the geometry of internal elements of the system, the distance between consecutive nodes of the grid ($P_{j,p}$) but largely uninfluenced by the structural properties of the connectors. The upper and lower frequency limits of this region (*UL* and *LL*) are indicated in Fig. 8, respectively, corresponding to 1.9 and 2.7 Hz. Beyond *UL* the situation reverts to a set of higher network modes and thereafter, a second plateau appears in the frequency range coincident with high-order antisymmetric individual segment modes; this pattern of consecutive "steps" defines a typical pattern for the behavior.

UL and *LL* limits can be also related to the frequency of antisymmetric second modes in the individual stays; the upper α is directly related to the frequency (wavelength) of shorter cables while the lower value is influenced by a combination of the stays in the central part of the structure (presence of pseudo-symmetric components [1]). The similarity of localized modes to antisymmetric individual cable eigenvectors is shown in Fig. 8, as an example, for mode 22, compared to its "modal origins" (second modes of AS15S, AS16 and AS18).

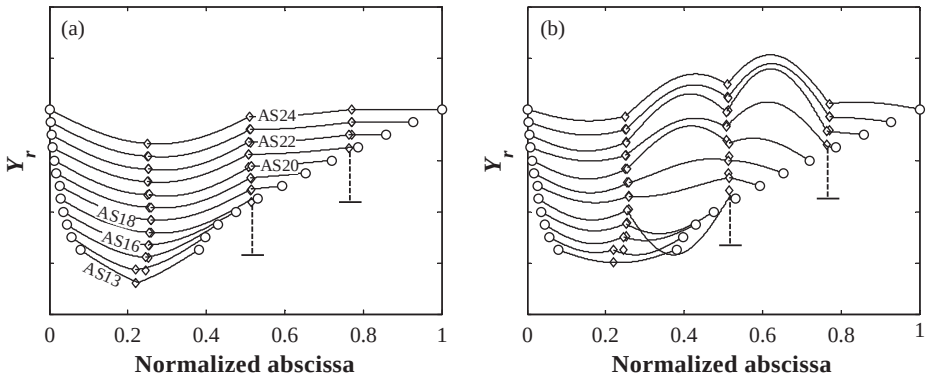

Fig. 9. Central-span unit of the Hartman Bridge with restrainers 2 and 3 extended to ground (NET_3CG). (a) 1st network mode NM1, $\alpha = 1.86$; (b) 2nd network mode NM2, $\alpha = 3.15$.

The use of rigid connectors (NET_3RC) does not introduce substantial qualitative modifications with respect to the original mode-frequency evolution in Fig. 8 (NET_3RC with rigid restrainers and the original NET_3C substantially overlap), suggesting that the real network can be modelled effectively with rigid connectors as concerns the transverse interaction among stays. As an example, the increment in the frequency of the fundamental mode is only about 3%. The overall action of progressively increasing the stiffness of the restrainers produces increments (although modest) in the frequency of the first global modes (and, to a lesser extent, of the higher global solutions) but no modifications in the modal behavior.

On the contrary, the presence of the ground connectors (restrainers 2,3) is able to modify only global modes (1 to 3, beyond 27), influencing the response at low frequencies (first modes) and, subsequently, only for solutions in a frequency range greater than 3 Hz. No variations in the intermediate modes (localized modes) on the plateau can be seen.

Fig. 9 depicts the modal eigenfunctions related to the first two fundamental modes of NET_3CG (ground connectors). The comparison with the equivalent solutions of the original configuration suggests that amplitudes are remarkably reduced in the portion of the stays connected to the deck (e.g., mode 1, Fig. 9) for purely symmetric modes. The same behavior is also observed for mode 2 (antisymmetric), in which the oscillations are mostly confined to a restricted region of the network (two or three columns of elements on the left side of the network).

3.2. *Introduction of modifications to the configuration and number of the restrainers*

The investigation in Section 3.1 was extended to the sensitivity of the system to geometrical variations in the configuration of the cross-ties. By preserving the structural properties of primary and secondary cables, the following examples were considered:

- NET_2C: two side connectors only; elimination of the central cross-tie (restrainer 2) from the original configuration (Fig. 4);
- NET_1C: one central connector only (Fig. 10(a));

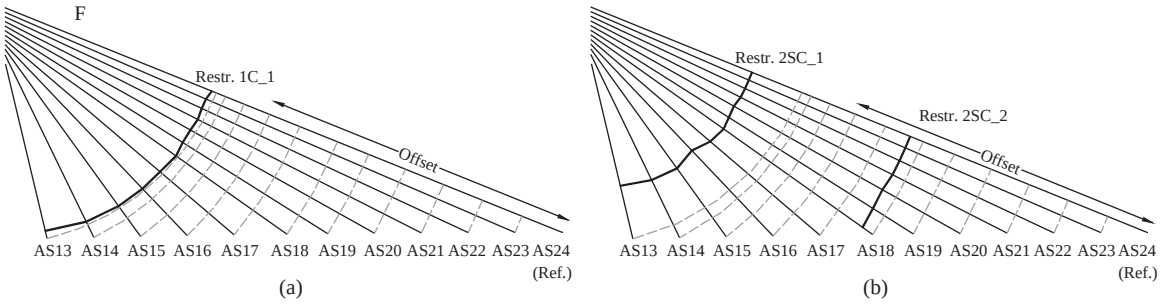

Fig. 10. Modified three-dimensional configurations for the central-span unit of the Fred Harman Bridge. (a) NET_1C, one single central connector; (b) NET_2SC, two symmetric restrainers.

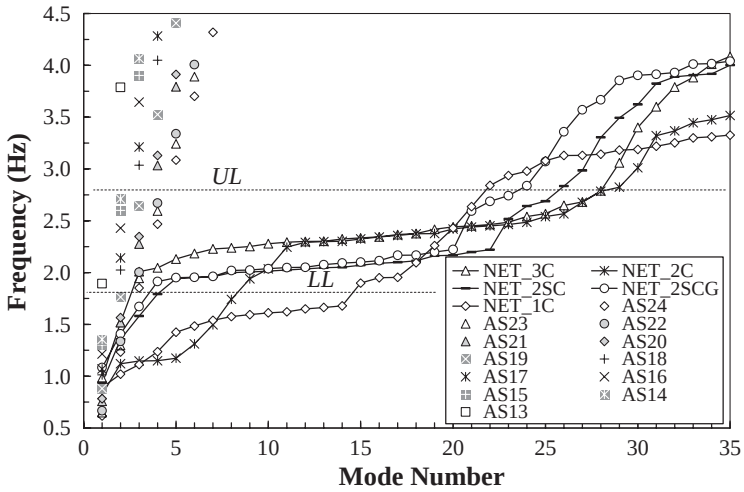

Fig. 11. Modified central-span unit of the Fred Hartman Bridge. Comparison of mode-frequency evolution curves: NET_3C (-△-), original configuration; NET_2C (-∗-) restrainers 1 and 3 only; NET_2SC (- – -) two symmetric ties; NET_2SCG (—○—) two symmetric ties with restrainers 2SC_2 extended to ground; NET_1C (-◇-) one central tie only (*UL* and *LL*, upper and lower limits of the plateau).

- NET_2SC: two almost symmetric connectors (restrainers 2SC_1 and 2SC_2, Fig. 10(b)), with optimized configuration to enhance regularity in the behavior;
- NET_2SCG: same as the previous case with additional extension to ground of cross-tie 2SC_2.

Fig. 11 presents the frequency-evolution chart summarizing the vibration characteristic of these examples and compared with the original configuration (NET_3C). For cases NET_2C and NET_1C, it can be seen that the new geometry of the network is responsible for a clear modification of the overall response. The reduction in the fundamental frequency can be quantified as 10–15% (0.8–0.85 Hz) with respect to the original configuration (0.98 Hz). The single plateau is split in two branches in case NET_2C. The first one is associated with a considerably lower frequency interval, which can be related to the behavior of antisymmetric modes (mode number 2) involving the longer cables (AS24, AS23); the second one is almost coincident with localized modes of the original configuration (modes 10–20), in terms of

frequency. This situation is potentially undesirable since it produces a fragmentation in the modal performance, with lower frequencies in the range of modes 1–10 with respect to the original design specifications. Moreover, this feature is repeated for higher modes (beyond 30) and subsequent groups of local modes. Also, network modes are affected: the frequency of the second global mode is lower than that of the corresponding component (antisymmetric, mode number 2) of the individual cables (also stay AS24). Moreover, selection of the distance between connectors has contributed to the development of a pseudo-symmetric behavior (the wavelength of these modal forms is principally affected by the relative position of the cross-ties on the central stays), concentrated in the intermediate elements of the longest cables.

When the example with one cross-tie is only analyzed (NET_1C, Fig. 10(a)), three different branches can be detected from Fig. 11. The location of the restrainer is fixed in this example by the geometry of the system in accordance with the requirement of simultaneous connection of all the stays. This configuration enhances the pseudo-symmetric response of the network, localized or global, which would be magnified by the introduction of an extension to ground. Another consequence is related to an earlier development of a second source of localized behavior, i.e., an extended plateau in the proximity of mode 20 (about 3 Hz), in comparison to the 4 Hz second plateau of the original configuration (NET_3C).

Good performance is achieved with the configuration NET_2SC (Fig. 10(b)), in which the location of the cross-ties is selected as symmetric with respect to cable AS22. The results of Fig. 11 for the simple case without additional element to ground (NET_2SC) show that frequencies and general patterns of the evolution function have positively increased for the fundamental modes. The subdivision into consecutive localized-mode regions has disappeared. The position of the plateau on the frequency axis is at about 1.9 Hz, almost the same as the original configuration (2.0–2.1 Hz); its extension on the mode number axis is shorter than that of NET_3C, suggesting a lower susceptibility to localized solutions with respect to the original configuration (approximately in the range of modes 5–20). Moreover, differences with the three-tie system frequencies tend to disappear for higher modes, beyond 3.5 Hz.

The insertion of a ground connector in correspondence with restrainer 2SC_2 produces, as expected, a frequency increment only for the first modes or network higher components, also evident from the study of Fig. 11. Moreover, in this case the computed fundamental frequency, about 1 Hz, is slightly higher than that of NET_3C, while it is lower for the second modal component. A more careful analysis of the fundamental modes revealed that the net distinction between localized and global eigenfunctions becomes less evident and not simply perceived from Fig. 11, since the pseudo-symmetric behavior [1] is emphasized by the presence of the secondary cable with extension to ground. Nevertheless, the benefits of a ground connector must be carefully evaluated with respect to the dynamic increment/decrement of the axial force in the cross-tie segments (either connecting two consecutive stays or the system to the deck) due to external excitation, along with the possibility of snapping/slackening of the wire ropes.

4. Experimental validation: study of the side-span cable arrangement of the Fred Hartman Bridge

Validation of the proposed approach was performed by the comparison of a specific study example with a set of experimental data. A long-term ambient vibration survey is currently in

progress on the Hartman Bridge [2,3] to monitor stay-cable vibration and to better understand the overall performance of the structure.

The methodology was applied to the study of the side-span unit of the south tower of the bridge. Fig. 12 shows the current configuration of the "A-line" 12-stay system (AS1–AS12) that was used in the present analysis; the cable network is configured by means of three transverse restrainers, similar to those presented in Section 3. The data set was extracted from the records of four in-plane and out-of-plane accelerometers, placed along stays AS1, AS3, AS5 and AS9 (Fig. 12(a)) at a height of approximately 7 m from the deck level. This analysis has also considered the results of a FEM simulation of the same network, developed in Ref. [7] by means of ANSYS53 code with 99 elements for each stay and used as the design basis of the currently installed system.

A parametric investigation of the network free-vibration problem solution patterns was performed in order to identify the geometric and physical parameters, primarily influencing the qualitative but also quantitative behavior of the system. Three classes of variables were recognized: frequencies of the individual stays, mechanical properties of the secondary cables, and mass of the restrainers and collars (neglected in the original formulation of Section 2.1).

The fundamental frequencies of stays AS1, AS3, AS5 and AS9 were identified from the available acceleration records before the installation of the network in 1998 and integrated through the results of a previous experimental campaign. These values were derived after careful statistical classification of the results, derived from the in-plane spectral analyses of a selected population of events. For the remaining cables, the quantities detected during an earlier measurement program were selected.

Table 2 presents the first mode frequencies of the 12 stays; measured values (subdivided between currently monitored cables and previous results) are also compared to the design quantities [7]. Significant differences can be seen between the two sets: lower measured frequencies for the longer cables (AS1–AS3), whereas higher values for AS7 and AS9–AS11 in the "high-frequency side" of the network. Preliminary parametric simulations suggested that the variability

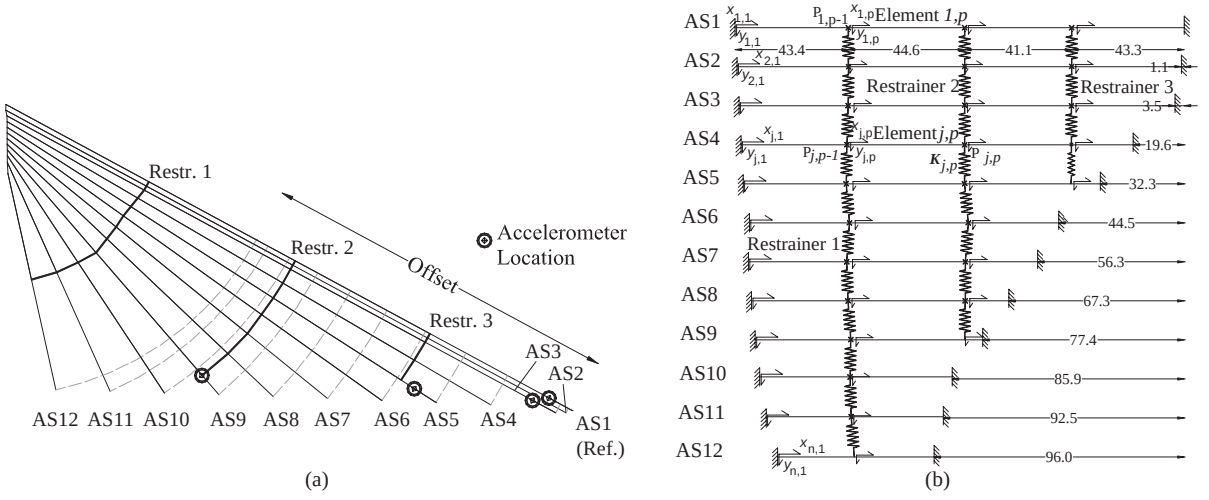

Fig. 12. Side-span unit of the Fred Hartman Bridge ("A-line"). (a) Three-dimensional network; (b) equivalent two-dimensional model. Measurements in meters; vertical units are not to-scale.

Table 2
AS1–AS12 side-span individual stays of the Hartman Bridge; first-mode fundamental frequency (Hz)

Stay	Measured values	Design values [7]	Difference (%)
AS1	0.626[a]	0.671	−6.7%
AS2	0.654[b]	0.686	−4.7%
AS3	0.615[a]	0.701	−12.3%
AS4	0.720[b]	0.715	+0.7%
AS5	0.790[a]	0.837	−5.6%
AS6	0.864[b]	0.882	−2.0%
AS7	1.000[b]	0.867	+15.3%
AS8	1.100[b]	1.124	−2.1%
AS9	1.246[a]	1.178	+5.8%
AS10	1.355[b]	1.259	+7.6%
AS11	1.613[b]	1.601	+0.7%
AS12	1.700[b]	1.799	−5.5%

[a] Monitored stays in this study.
[b] Derived from previous measurement.

of the predicted network frequencies can be significant. In some cases, such differences can be assumed as 6–7% of the reference values if the stay frequencies are allowed to vary between 10% and 15% with respect to design specifications (as sometimes detected in Table 2).

The modulus of elasticity of the secondary system was selected as $E = 1.65 \times 10^{11}$ N/m^2 on the network modes, and accounting for the potential variability of the effective E for non-primary wire ropes (as suggested in Ref. [8]).

The mass of the cross-ties and corresponding collars on the twelve stays, not modelled in Ref. [1], was also incorporated for comparison purposes with not only the experimental results but also the available FEM simulations. A lumped system was used; details can be found in Appendix A. Parametric values were determined from the design specifications [7]. It is worth emphasizing that a decrement of modal frequencies was noticed due to mass effects alone: neglecting of this contribution can lead to network frequency overestimates (about 1%).

The frequencies of the predicted network modes, derived from measured stay frequencies (PNM_M) and design values (PNM_D), are summarized in Table 3 (most significant modes between 0 and 3.5 Hz), along with the first three network modes, available from the FEM simulation [7]. A classification in terms of subdivision into global and localized network modes, symmetric and antisymmetric, is also indicated.

A general frequency decrement in the fundamental network modes (e.g., NM1–NM3) can be detected between PNM_M and PNM_D, due to the different set of frequencies (Table 2); this tendency seems to be opposite in the case of those localized modes (e.g., NM29 and NM30) concentrated in the lower portion of the system (Fig. 12) where higher frequencies were measured. The fundamental frequency (NM1), computed through the experimental set of values (PNM_M in Table 3) is 0.905 Hz, potentially susceptible to deck-stay interaction with the 10th bending mode of the bridge (0.924 Hz, [6]). The plateau behavior (localized modes) was detected between NM4 (2.3 Hz) and NM30 (3 Hz).

Table 3
"A-line" side-span system. Frequencies (Hz) of the predicted network modes, derived from measured stay frequencies (PNM_M) and design values (PNM_D); comparison with the results of a finite-element simulation (FEM) [7]

Mode	NM1	NM2	NM3	NM4	NM5	…	NM29	NM30	NM31	NM32	NM33
PNM_M	0.905	1.408	1.972	2.274	2.340	…	2.981	3.063	3.197	3.284	3.345
PNM_D	0.916	1.468	2.033	2.127	2.284	…	2.959	3.032	3.231	3.311	3.444
FEM	0.886	1.443	2.030	—	—	…	—	—	—	—	—
Mode type	GS	GAS	G-S	L	L	…	L	L	GS	GS	L

(G) Global network mode; (L) local network mode; (S) symmetric; (AS) anti-symmetric.

The comparison with the FEM was performed with respect to the set of design frequencies (PNM_D), perhaps more consistent with the input variables used in Ref. [7]. The results are practically coincident for NM2 and NM3; a difference of +3% can be noticed in the first mode predicted frequency (0.916) with respect to the finite-element analysis (0.886). Differences are most probably connected to the incomplete information on the physical quantities adopted by the FEM (this information is unavailable to the authors).

The correspondence between the predicted modal characteristics based upon the measured frequencies (PNM_M in Table 3) and the real behavior was carried out by simultaneous spectral analysis of the in-plane acceleration record database of the four locations, after the installation of the restrainers. The analysis was founded on the simultaneous identification of the same dominant in-plane frequency on all the four investigated cables (comparison of the in-plane acceleration power spectral density, PSD_{a-y}). More than 2000 trigger files from year 2000–2001 were analyzed (after the installation of the restrainers). The investigation considered the presence of cable network behavior along with individual cable and, eventually, global (deck) structure modes.

The experimental identification of network modes (Table 3, PNM_M) was restricted to a subset of "visible" components in accordance with the location of the accelerometers, since predicted localized modes, concentrated in the central and upper portion of the system, could not be physically detected.

Simultaneous peak amplitudes in the acceleration spectra from the stays were found in a significant number of realizations in the frequency range between 1.37 and 1.38 Hz, corresponding to the simulated frequencies of the second global antisymmetric mode (1.41 Hz in Table 3, PNM_M), and in the range of 3.25–3.27 Hz, associated with higher global symmetric modes (i.e., NM32, predicted at 3.29 Hz in Table 3). Differences between experiments and predictions are within the numerical approximation error (1%). NM3 is also perceived to be present in few occasions at 2.07 Hz (1.97 in Table 3, PNM_M).

A relevant example is concerned with record H02236, corresponding to a 5-min portion of an extreme event. Fig. 13 shows the corresponding PSD_{a-y}, extracted from the five-minute time history, subdivided in the intervals 0.5–1.0 Hz (a), 1.0–1.5 Hz (b), 2.0–2.75 Hz (c) and 2.75–3.5 Hz (d). The global structure (below 3 Hz, Ref. [7]) and individual stay modal frequencies are also indicated. A different vertical axis scale was employed in the figures to enhance the readability of the plots.

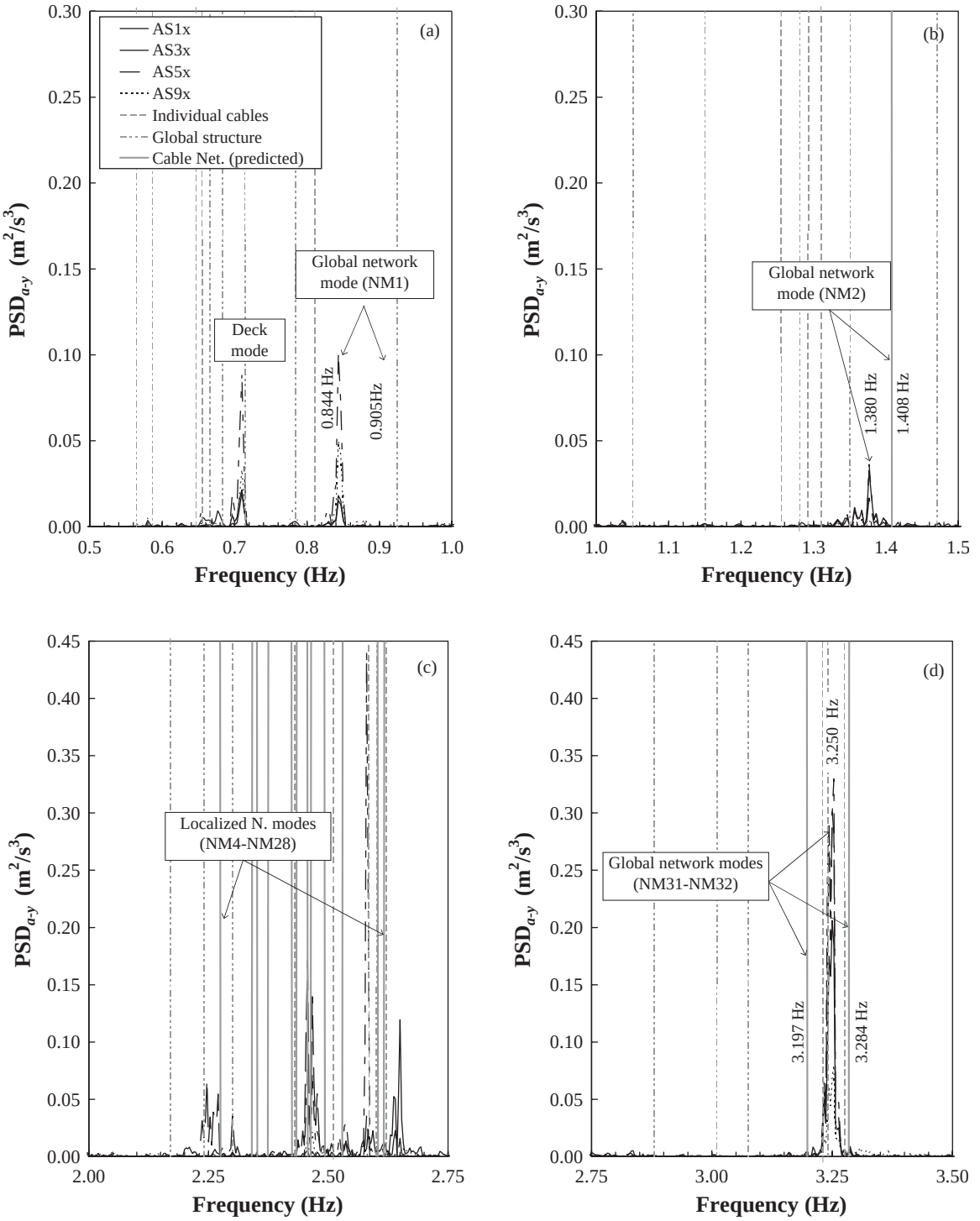

Fig. 13. Fred Hartman— "A-line" side span. Comparison of the power spectral density of the in-plane acceleration (PSD_{a-z}) recorded on stays AS1, AS3, AS5, AS9 with the predicted network frequencies (record H02236). (a) 0.5–1.5 Hz; (b) 1.0–1.5 Hz; (c) 2.0–2.75 Hz; (d) 2.75–3.5 Hz.

A first alignment of the four peaks occurs at 0.84–0.85 Hz (Fig. 13(a)) and is considered the first global mode of the network; this compares with the predicted value of 0.905 Hz (PNM_M). This is the only event (along with 2–3 subsequent records, corresponding to a duration of approximately 20 min), in which NM1, as network mode, was clearly identified. This extremely rare event was mainly driven by the high-amplitude motion of the deck due to vortex shedding and related to a strong wind with direction almost perpendicular to the bridge axis. A noticeable peak at 0.71 Hz (8th vertical mode of the deck structure) is in fact present as shown in Fig. 13(a). Differences between the experimental and predicted frequency seem quite large in this case (6–7%). Nevertheless, a similar observation also applies if the design values of the cable frequencies or the FEM simulations are considered, suggesting that this difference is due to factors also not captured with alternative techniques or input data.

Uncertainties in the identification of the model parameters, background noise, influence of geometry and cable sag (recently explored in Ref. [9] in the case of two parallel cables with one restrainer), amplitude-dependence effects neglected in the current method, along with non-stationary patterns in the selected records (complicating the interpretation of an "averaged" spectral result), may be in part responsible for such differences. Moreover, time dependence of the cable tension is evident from the records (long-term frequency diminution, in particular for the longest and most excited stays); predictions are founded on measured frequency values, only possible before the installation of the restrainers (1997), while the spectral modal identification is derived from the analysis of years 2000 and 2001.

In addition, external boundary conditions (fixed supports) of the partial differential equation system [1] are believed to be potentially violated in this mode, in which towers are speculated to be experiencing low-frequency oscillations. Large-amplitude motion of these sub-elements of the structure is likely to induce a decrement of relative distance between corresponding cable ends with consequent reduction of the fundamental frequency. Extensional symmetric modes (such as NM1), where the contribution of the cable tension predominates in the definition of the modal characteristics, can be significantly affected by such "imperfect" boundary conditions. This observation seems to be consistent with the very good agreement between full-scale data and predictions that is recorded for NM2 (antisymmetric), in which the geometry alone is primarily responsible for the modal configuration (i.e., a non-extensional mode).

In Fig. 13(b), another simultaneous alignment of the spectra on three cables can be seen at 1.38 Hz, coincident with the second mode of the network, NM2. This mode is antisymmetric and, accordingly, the response of AS9, located in correspondence with the central axis of the network, is excluded. In both cases (Fig. 13(a) and (b)), the frequencies are clearly associated with new modal forms (individual cable frequencies of AS1, AS3, AS5 and AS9 are in fact absent).

In Fig. 13(d), NM31, the fourth global mode of the system, can be observed (3.22 Hz) and compared to the predictions. Indication of the potential development of local network modes rather than individual stay oscillation can be noticed in Fig. 13(c). Localized modes, potentially detectable by the sensors in accordance to their location, are concentrated between 2.3 and 2.6 Hz, while they tend to disappear in other ranges. Despite the presence of predicted frequencies associated with individual cable behavior in this region, patterns of observed frequencies were not consistent with unrestrained stay oscillation.

This investigation, while illuminating, cannot be considered comprehensive since the experimental system was not designed for this purpose and an extension of the instrumentation

to other stays or locations was not possible. It is also worth mentioning that the challenges of long-term monitoring of such a complex system are significant [2,3,6]. Moreover, most ambient-induced vibration phenomena are concentrated in selected portions of the bridge (e.g., groups of stays), where localized modes are more likely to be detected with respect to global modes and relatively high-oscillation amplitudes are usually required for the appropriate identification.

5. Conclusions

Limited investigations of in-plane vibrations of large cable networks are available in the literature. An alternative methodology for the analytical derivation of the equation of motion (free-vibration problem) of a network, based on the taut-cable theory, developed in a companion paper for simplified cases [1], has been extended and applied to the study of a real case. Advantages and limitations with respect to finite-element simulations are addressed in Section 7 of Ref. [1].

The central and side span configurations of the Fred Hartman Bridge (Texas, USA) were considered in this study. The analyses highlighted the distinction between "global" and "localized" mode shapes of the network. Subsequently, a sensitivity analysis of the central-span network arrangement was carried out to examine the influence of geometry and configuration modifications on these systems.

The methodology was also compared to experimental results derived from an intensive ambient vibration survey on the same bridge. Correspondence between predicted values and measured quantities was found. Data records confirmed the existence of global or localized system modes and contributed to the validation of the procedure.

The results suggest that the control of this category of structures can become very challenging at higher frequencies, potentially reducing the overall performance, due to the different nature of the modes: the frequency and modal mass increment in the fundamental modes must be balanced with the potential undesirable behavior of the localized modes.

Acknowledgements

The authors would like to acknowledge the contribution of the sponsors for the work described in this and the companion paper [1]. This effort has also been supported through an FHWA-sponsored project (Harold Bosch technical contact) on stay-cable vibration awarded to a team of investigators including HNTB Corporation, New York, Johns Hopkins University, Baltimore, Maryland, Rowan Williams, Davies and Irwin, Ontario, Canada, and Buckland and Taylor of Vancouver, BC, Canada. This support, as well as the ideas and comments from members of the research team are also gratefully acknowledged. This research was motivated by the second author's involvement in a number of field projects investigating this problem over the past 5 years including the East Huntington Bridge (funded by the West Virginia Department of Transportation through Modjeski and Masters of Harrisburg, Pennsylvania), and the Fred Hartman and Veterans' Memorial Bridges, funded by the Texas Department of Transportation through Texas Tech University and the University of Texas at Austin, in a project managed by Whitlock, Dalrymple Poston and Associates, Inc. of Austin, Texas.

Appendix A. Equilibrium boundary conditions

The mass of the secondary system in Section 4 (transverse cables and anchorages to the primary stays) was simulated by means of a lumped-element configuration, $M_{j,p}$, concentrated in correspondence with the $P_{j,p}$ nodes of the network (Fig. 1). The equilibrium boundary conditions (8) and (9), incorporating the inertial force contribution associated with each $M_{j,p}$ (or, equivalently, through the dimensionless quantities $\chi_{j,p} = M_{j,p}/(\mu_1 L_1)$), can be rewritten as

$$K_{j,p}(B_{j+1,p+1} - B_{j,p+1}) = \sum_{k=1}^{j} \frac{\alpha\pi H_1}{L_1}\sigma_{k,j}^{p} \times \left\{ \begin{array}{c} v_k[A_{k,p}\cos(\alpha\pi f_k \xi_{k,p}) - B_{k,p}\sin(\alpha\pi f_k \xi_{k,p}) - A_{k,p+1}] \\ -\alpha\pi\chi_{k,p}B_{k,p+1} \end{array} \right\} \quad \text{with } p = 1, \ldots, \tilde{m}-1,\ j = 1, \ldots, (g_p - 1),\ \tilde{m} = \max[g_p], \tag{A.1}$$

$$K_{G_p}B_{g_p,p+1} = \sum_{j=1}^{g_p} \frac{\alpha\pi H_1}{L_1}\sigma_{j,g_p}^{p} v_j \times \left\{ \begin{array}{c} v_j[A_{j,p}\cos(\alpha\pi f_j \xi_{j,p}) - B_{j,p}\sin(\alpha\pi f_j \xi_{j,p}) - A_{j,p+1}] \\ -\alpha\pi\chi_{j,p}B_{j,p+1} \end{array} \right\} \quad \text{with } p = 1, \ldots, \tilde{m}-1. \tag{A.2}$$

References

[1] L. Caracoglia, N.P. Jones, In-plane dynamic behavior of cable networks. Part 1: formulation and basic solutions, *Journal of Sound and Vibration* 279 (2005) 969–991.

[2] E. Ozkan, J.A. Main, N.P. Jones, Investigation of cable-deck interaction using full-scale measurements on a cable-stayed bridge, *Proceedings of the First Americas Conference on Wind Engineering* (*AAWE*), Clemson University, Clemson, SC, 2001.

[3] E. Ozkan, J.A. Main, N.P. Jones, Full-scale measurements on the Fred Hartman Bridge, *Journal of Wind Engineering* 89 (2001) 553–556.

[4] A.M. Abdel-Ghaffar, M.A. Khalifa, Importance of cable vibration in dynamics of cable-stayed bridges, *American Society of Civil Engineers, Journal of Engineering Mechanics* 117 (1991) 2571–2589.

[5] N.J. Gimsing, *Cable Supported Bridges; Concept and Design*, Wiley, New York, 1983.

[6] E. Ozkan, J.A. Main, N.P. Jones, Long-term measurements on a cable-stayed bridge, *Proceedings of the IMAC-XIX Conference*, Orlando, FL, 2001.

[7] Whitlock, Dalrymple, Poston & Associates, Inc., Evaluation and repair of stay-cable vibrations of Fred Hartman Bridge and Veterans Memorial Bridge, Report 1, Texas Department of Transportation, 8th January 1998.

[8] H.M. Irvine, *Cable Structures*, MIT Press, Cambridge, 1981.

[9] H. Yamaguchi, Md. Alauddin, Control of cable vibrations using secondary cable with special reference to nonlinearity and interaction, *Engineering Structures* 25 (2003) 801–816.